Title: Redox potential as a master variable controlling pathways of metal reduction by *Geobacter sulfurreducens*

Running Title: Fe(III) reduction by *G. sulfurreducens*

Authors: Caleb E. Levar[1], Colleen L. Hoffman[2], Aubrey J. Dunshee[2], Brandy M. Toner[2, 3], Daniel R. Bond[1]

Author Affiliations: 1) BioTechnology Institute, Department of Microbiology, University of Minnesota - Twin Cities, St. Paul, MN 55108, USA
2) Department of Earth Sciences, University of Minnesota – Twin Cities, Minneapolis, MN, 55455, USA
3) Department of Soil, Water, and Climate, University of Minnesota – Twin Cities, St. Paul, MN 55108, USA

Corresponding Author:
Daniel R. Bond
140 Gortner Laboratory
1479 Gortner Ave
St. Paul, MN 55108
dbond@umn.edu

Conflict of Interest Statement: The authors declare no conflict of interest.

Subject Category: Geomicrobiology and microbial contributions to geochemical cycles

Keywords: Metal reduction, Extracellular electron transfer, Iron oxide, *Geobacter*

Abstract:

Geobacter sulfurreducens uses at least two different pathways to transport electrons out of the inner membrane quinone pool before reducing acceptors beyond the outer membrane. When growing on electrodes poised at oxidizing potentials, the CbcL-dependent pathway operates at or below redox potentials of -0.10 V vs. the Standard Hydrogen Electrode (SHE), while the ImcH-dependent pathway operates only above this value. Here, we provide evidence that *G. sulfurreducens* also requires different electron transfer proteins for reduction of a wide range of Fe(III)- and Mn(IV)- (oxyhydr)oxides, and must transition from a high- to low-potential pathway during reduction of commonly studied soluble and insoluble metal electron acceptors. Freshly precipitated Fe(III)-(oxyhydr)oxides could not be reduced by mutants lacking the high potential pathway. Aging these minerals by autoclaving did not change their powder X-ray diffraction pattern, but restored reduction by mutants lacking the high-potential pathway. Mutants lacking the low-potential, CbcL-dependent pathway had higher growth yields with both soluble and insoluble Fe(III). Together, these data suggest that the ImcH-dependent pathway exists to harvest additional energy when conditions permit, and CbcL switches on to allow respiration closer to thermodynamic equilibrium conditions. With evidence of multiple pathways within a single organism, the study of extracellular respiration should consider not only the crystal structure or solubility of a mineral electron acceptor, but rather the redox potential, as this variable determines the energetic reward affecting reduction rates, extents, and final microbial growth yields in the environment.

45 **Introduction:**

46 Fe(III)-(oxyhydr)oxides can exist in at least 15 mineral forms with variable physiochemical
47 properties that span a wide range of formal oxidation-reduction (redox) midpoint potentials (Majzlan,
48 Navrotsky, & Schwertmann, 2004; Majzlan, 2011, 2012; Nealson & Saffarini, 1994; Schwertmann &
49 Cornell, 2000; Thamdrup, 2000). The electron-accepting potential of any given Fe(III)-(oxyhydr)oxide
50 structure is not a fixed value, and becomes less favorable with increasing crystallinity, particle size, pH,
51 or ambient Fe(II) concentration (Majzlan, 2012; Navrotsky, Mazeina, & Majzlan, 2008; Sander,
52 Hofstetter, & Gorski, 2015; Thamdrup, 2000). Differences in effective redox potential alters the energy
53 available to be captured by bacteria able to couple the oxidation of an electron donor to reduction of
54 these minerals (Flynn, O'Loughlin, Mishra, DiChristina, & Kemner, 2014; Thauer, Jungermann, & Decker,
55 1977). Because of this structural and environmental diversity, organisms able to reduce metals could
56 sense the energy available in their electron acceptors and utilize different electron transfer pathways,
57 similar to how *E. coli* uses distinct terminal oxidases in response to levels of available oxygen (Green &
58 Paget, 2004; Russell & Cook, 1995).

59 One well-studied dissimilatory metal reducing organism, *Geobacter sulfurreducens*, can grow via
60 reduction of metal (oxyhydr)oxides ranging in predicted midpoint redox potential from +0.35 V vs. the
61 Standard Hydrogen Electrode (SHE)(e.g., birnessite, ca. $Na_xMn_{2-x}(IV)Mn(III)_xO_4$, x ~ 0.4) to -0.17 V vs. SHE
62 (e.g., goethite, α-FeOOH) (Caccavo et al., 1994; Majzlan et al., 2004; Majzlan, 2012; Post & Veblen, 1990;
63 Thamdrup, 2000). Recent work examining electron transfer from *G. sulfurreducens* to poised graphite
64 electrodes demonstrated that this organism uses at least two different inner membrane electron
65 transfer pathways, known as the CbcL- and ImcH-dependent pathways (Levar, et al., 2014; Zacharoff, et
66 al., 2016). The 'low' potential, CbcL-dependent pathway, is required for growth with electrodes at or
67 below potentials of -0.10 V vs. SHE, while the 'high' potential, ImcH-dependent pathway, is essential

68 when electrodes are poised at redox potentials above this value. As mutants lacking each pathway only
69 grow with electrodes poised above or below these thresholds, cells containing only CbcL or ImcH might
70 also be able to be used as 'sensors' to report the redox potential of an extracellular electron acceptor
71 such as a metal (oxyhydr)oxide. As it is difficult to determine the effective redox potential of these
72 minerals (Sander et al., 2015), such information could aid laboratory characterization, and provide
73 evidence that bacteria use different pathways for different metals in the environment.

74 The discovery of multiple inner membrane pathways is based on work with electrodes held at
75 constant potentials, but poses many questions regarding *G. sulfurreducens'* interactions with more
76 complex mineral substrates. Does the organism transition from one pathway to the other as simple
77 environmental factors such as Fe(II):Fe(III) ratios alter redox potentials? Do manipulations known to
78 alter redox potential, such as pH or particle size, also influence the pathway utilized? As this +/- 0.5 V
79 redox potential range represents nearly 50 kJ per mol of electrons transferred, do different electron
80 transfer mechanisms allow higher yield of this microbe?

81 Here, we demonstrate that *G. sulfurreducens* requires both the CbcL- and the ImcH-dependent
82 electron transfer pathways for complete reduction of a variety of Fe and Mn minerals. By using mutants
83 only able to function above or below specific redox potentials, we show that minerals often used for
84 study of extracellular electron transfer begin as 'high' potential electron acceptors reducible by the
85 ImcH-dependent pathway, but transition during reduction to 'low' potential electron acceptors requiring
86 the CbcL-dependent pathway. Simple variations in mineral handling such as autoclaving, or pH changes
87 that alter redox potential by 30 mV, can alter the electron transfer pathway required by the organism,
88 further showing that bacteria respond to subtle changes in mineral redox potentials. These data
89 highlight the complexity of studying growth with minerals, and suggests that the proteins used for

90 electron flow out of *G. sulfurreducens* are more strongly influenced by redox potential than the crystal
91 structure, aggregation behavior, or even solubility of the terminal acceptor.

92

93 **Materials and methods:**

94 **Bacterial strains and culture conditions:** Strains of *Geobacter sulfurreducens* used in this study
95 are described in Table 1. All strains were routinely cultured from freezer stocks stored at -80 degrees
96 Celsius, separate colony picks from agar plates were used to initiate replicate cultures used in all
97 experiments. Strains were cultured in NB minimal medium composed of 0.38 g/L KCl, 0.2 g/L NH_4Cl,
98 0.069 g/L $NaH_2PO_4 \cdot H_2O$, 0.04 g/L $CaCl_2 \cdot 2H_2O$, and 0.2 g/L $MgSO_4 \cdot 7H_2O$. 10 ml/L of a chelated mineral mix
99 (chelator only used for routine growth with soluble acceptors, see below) containing 1.5g/L NTA, 0.1 g/L
100 $MnCl_2 \cdot 4H_2O$, 0.3 g/L $FeSO_4 \cdot 7H_2O$, 0.17 g/L $CoCl_2 \cdot 6H2O$, 0.1 g/L $ZnCl_2$, 0.04 g/L $CuSO_4 \cdot 5H2O$, 0.005 g/L
101 $AlK(SO_4)_2 \cdot 12H_2O$, 0.005g/L H_3BO_3, 0.09 g/L Na_2MoO_4, 0.12 g/L $NiCl_2$, 0.02 g/L $NaWO_4 \cdot 2H2O$, and 0.1 g/L
102 Na_2SeO_4 was also added. Fumarate (40 mM) was used as an electron acceptor for growth of initial stocks
103 picked from colonies, and acetate (20 mM) was used as the sole electron and carbon source. Unless
104 otherwise noted, the pH of the medium was adjusted to 6.8 and buffered with 2 g/L $NaHCO_3$, purged
105 with N_2:CO_2 gas (80%/20%) passed over a heated copper column to remove trace oxygen, and
106 autoclaved for 20 minutes at 121 degrees Celsius.

107 **Here Table 1**

108 **Growth of *G. sulfurreducens* with Fe(III)-citrate and continuous redox potential monitoring-**

109 Minimal medium containing 20 mM acetate as the carbon and electron donor and ~80 mM Fe(III)-citrate
110 as the electron acceptor was added to sterile bioreactors constructed as previously described, using
111 both working and counter electrodes bare platinum wire approximately 2 cm in length. The headspace
112 of each reactor was purged with anaerobic and humidified N_2:CO_2 (80%/20%) gas. Calomel reference

113 electrodes were used, and a solution of 0.1 M $NaSO_4$ stabilized with 1% agarose separated from the
114 medium by a vycor frit provided a salt bridge between the reference electrode and the growth medium.
115 The working volume of the bioreactors was 15 ml. A 16-channel potentiostat (VMP; Bio-Logic, Knoxville,
116 TN) using the EC-lab software (v9.41) was used to measure the open circuit voltage between the
117 working and reference electrode every 500 seconds, providing a continuous readout of the redox
118 potential in the medium. After redox potential was stable for at least 5 hours, stationary phase cells
119 were added to each bioreactor at a 1:100 v/v inoculum size and the change in redox potential was
120 measured over time. When co-cultures were used, and equal volume of cells was added for each strain
121 (i.e., 1:100 each of Δ*cbcL* and Δ*imcH* was added after the voltage was stable).

122 **X-ray diffraction (XRD) measurements:** Approximately 0.2-0.5 g of untreated bulk mineral
123 sample or 2.5 ml of mineral suspension in medium were analyzed by powder XRD. Minerals in basal
124 media were separated from suspension by filtration (0.22 µm) in an anaerobic chamber (Coy Laboratory
125 Products) under a N_2:CO_2:H_2 (75%:20%:5%) atmosphere, and stored in sealed mylar bags at -20 degrees
126 Celsius prior to analysis. Diffractograms were measured from using 20° to 89° (2Θ) range, a step size of
127 0.02 2Θ, and a dwell of 0.5°/minute using a Rigaku MiniFlex ASC-6AM with a Co source. The resulting
128 diffractograms were background subtracted, and phases were identified using Jade v9.1 software (MDI,
129 Inc.).

130 **Preparation of Fe(III)-(oxyhydr)oxides: "**Poorly crystalline FeO(OH)" was produced after Lovley
131 and Phillips, 1986, by adding 25% NaOH dropwise over 90 minutes to a rapidly stirring 0.4 M solution of
132 $FeCl_3$ until the pH was 7.0. The solution was held at pH 7.0 for one hour, and the resulting suspension
133 was washed with one volume of de-ionized and distilled water and used immediately (<24 after
134 synthesis) for XRD analysis and growth studies as rapid aging of such products to more crystalline
135 minerals (e.g., goethite) has been observed even when kept in the dark at 4 degrees Celsius (Raven, Jain,

136 & Loeppert, 1998). The resulting mineral prior to its addition to medium and autoclaving ("untreated
137 mineral") was identified as akaganeite (β-FeOOH) by powder X-ray diffraction. Washing this "untreated
138 mineral" samples with up to three additional volumes of de-ionized and distilled water did not change
139 the XRD pattern of the mineral or the reduction phenotypes observed. For all minerals, "untreated"
140 refers to the mineral suspension in MiliQ water prior to addition to medium and autoclaving, "fresh"
141 refers to the mineral suspension in medium, and "autoclaved" samples result from adding the
142 "untreated" minerals to medium and autoclaving (ie, autoclaving the "fresh" samples).

143 Goethite and 2-line ferrihydrite (ca. $Fe_{10}O_{14}(OH)_2$) (Michel et al., 2007) were synthesized after
144 Schwertmann and Cornell, 2000, with some modifications. For goethite, a solution of $FeCl_3$ was
145 precipitated through neutralization with 5 N KOH, and the resulting alkaline mineral suspension was
146 aged at 70 degrees Celsius for 60 hours to facilitate goethite formation. The suspension was then
147 centrifuged, decanted, and washed with de-ionized and distilled water prior to freeze drying. For 2-line
148 ferrihydrite, a solution of $FeCl_3$ was neutralized with KOH until the pH was 7.0. Suspensions were rinsed
149 with de-ionized and distilled water and either freeze dried or centrifuged and suspended in a small
150 volume of de-ionized and distilled water to concentrate the final product. Freeze dried samples yielded
151 XRD patterns indicative of 2-line ferrihydrite, but suspension of hydrated samples in growth medium
152 had an altered XRD pattern more similar to that of akaganeite. Freeze dried samples were stored at -80
153 degrees Celsius prior to addition to growth medium, while hydrated samples were used within 24 hours
154 of synthesis.

155 Schwertmannite ($Fe_8O_8(OH)_6(SO_4)\cdot nH_2O$) was synthesized using a rapid precipitation method
156 involving the addition of a 30% solution of H_2O_2 to a solution of $FeSO_4$ (Regenspurg, Brand, & Peiffer,
157 2004). The mixture was stirred rapidly for at least 12 hours until the pH was stable, at ~2.35. The solids
158 were allowed to settle for 1 hour, and the supernatant carefully decanted. Solids were washed by

159 centrifuging at 3,700 x g and suspending in 1 volume of de-ionized and distilled water. The product was
160 concentrated by a final centrifugation at 3,700 x g for 5 minutes and resuspension in 1/20 the initial
161 volume. XRD identified this initial product as schwertmannite, though subsequent addition to media at
162 neutral pH values and autoclaving rapidly altered the mineral form.

163 **Iron reduction assays:** Basal media were prepared as above with some modifications. Fumarate
164 was omitted as the Fe(III)-(oxyhydr)oxides were desired as the sole electron acceptor. NTA free trace
165 mineral mix (in which all components were first dissolved in a small volume of HCl) was used in order to
166 eliminate exogenous chelating compounds from the media. All media were purged with N_2:CO_2 gas
167 (80%:20%) passed over a heated copper column to remove trace oxygen. Where indicated, media were
168 autoclaved for 20 minutes at 121 degrees Celsius on a gravity cycle, and were immediately removed to
169 cool at room temperature in the dark. As is standard for *G. sulfurreducens* medium containing Fe(III)-
170 (oxyhydr)oxide (Caccavo et al., 1994), additional $NaH_2PO_4 \cdot H_2O$ (to a final concentration of 0.69 g/L) was
171 added prior to autoclaving, as more recalcitrant and less reducible forms of Fe(III)-(oxyhydr)oxide will
172 form when autoclaved without additional phosphate. For fresh akaganeite and 2-line ferrihydrite, 1 ml
173 of the Fe-(oxyhydr)oxide suspension was added to 9 ml of basal medium. The final pH was adjusted by
174 altering the pH of the basal medium prior to mineral addition and by altering the concentration of
175 $NaHCO_3$ used prior to purging with anaerobic N_2:CO_2 gas (80%/20%). For goethite, an 88 g/L suspension
176 was made in de-ionized and distilled water and 1 ml of this suspension was added to 9 ml of basal
177 medium. The resulting medium had an effective Fe_{total} concentration of ~20 mM as determined by fully
178 reducing an acidified sample with hydroxylamine and measuring the resulting Fe(II) using a modified
179 Ferrozine assay (Lovley & Phillips, 1987). Because the synthesis of schwertmannite results in an acidic
180 product below the pH at which *G. sulfurreducens* grows optimally (Caccavo et al., 1994; Regenspurg et
181 al., 2004), the mineral suspension was added to the basal medium (1:9) and the pH of the solution was

182 adjusted with NaOH and bicarbonate to produce a final pH of 6.8. For freeze dried 2-line ferrihydrite, 0.2
183 grams of freeze dried sample was added per 10 ml of basal medium.

184 In all cases, 100 µl of electron acceptor-limited stationary phase cells (OD_{600} = 0.55) grown from
185 single colony picks in NB basal medium containing acetate (20 mM) and fumarate (40 mM) were used to
186 inoculate the Fe(III)-(oxyhydr)oxide containing media, with acetate provided as the electron and carbon
187 donor and the Fe(III)-(oxyhydr)oxide as the sole electron acceptor.

188 For all Fe(III)-(oxyhydr)oxide incubations except those involving goethite, a small sample was
189 removed at regular intervals and dissolved in 0.5 N HCl for at least 24 hours at 23-25 degrees Celsius in
190 the dark before the acid extractable Fe(II) present in the sample was measured. For incubations with
191 goethite, samples were incubated in 1 N HCl at 65 degrees Celsius for at least 24 hours in the dark,
192 followed by centrifugation at 13,000 x g for 10 minutes to remove solids. Fe(II) in the supernatant was
193 then measured.

194 **Manganese reduction assays:** Birnessite ($Na_xMn_{2-x}(IV)Mn(III)_xO_4$, x ~ 0.4) was prepared using the
195 protocol described in Chan, et al, 2015. Briefly, a solution of $KMnO_4$ was added to an equal volume of
196 $MnCl_2{\cdot}4H_2O$ solution and mixed vigorously. Solids were allowed to settle, and the overlaying liquid was
197 decanted off. The resulting solid was washed in de-ionized and distilled water and concentrated by
198 centrifugation. This suspension was added (~20mM) to basal medium containing acetate (10 mM) as the
199 carbon and electron donor. Cells were inoculated to a calculated OD_{600} of 0.005 from electron acceptor-
200 limited stationary phase cells. Mn(II) was measured indirectly as previously described (Chan et al., 2015;
201 Levar et al., 2014). Briefly, samples were acidified in 2 N HCl with 4 mM $FeSO_4$ added and allowed to
202 dissolve overnight at 25 degrees Celsius in the dark. After all solids were dissolved, the Fe(II)
203 concentration was measured. Because the reduction of Mn(IV) by Fe(II) is thermodynamically favorable,
204 the measured Fe(II) concentration can be used to extrapolate the Mn(II) present a given sample. When

205 measured Fe(II) concentrations are high, this implies that Mn(IV) concentrations are low (ie, Mn(IV) has
206 been reduced by the bacterial culture).

207 **Results:**

208 The inner membrane multiheme cytochromes ImcH and CbcL are implicated in transfer of
209 electrons out of the quinone pool when electron acceptors fall within different redox potential windows
210 (Levar et al., 2014; Zacharoff et al., 2016), though it is important to note that direct roles for ImcH and
211 CbcL in the movement of electrons out of the quinone pool have not been demonstrated. Mutants
212 lacking *imcH* are only able to reduce poised electrodes with 'low' redox potentials (≤ -0.10 V vs. SHE),
213 and are deficient in reduction of electrodes at redox potentials above this value (Levar et al., 2014). In
214 contrast, *cbcL* mutants have the opposite phenotype, reducing electrodes with relatively high electrode
215 redox potentials, and having a deficiency in reduction of electrodes at or below -0.10 V vs. SHE
216 (Zacharoff et al., 2016). The genes for ImcH and CbcL are constitutively expressed (Zacharoff et al.,
217 2016), yet use of each pathway appears to switch on or off in a matter of minutes during sweeps of
218 increasing or decreasing potential known as catalytic cyclic voltammetry (Marsili, Rollefson, Baron,
219 Hozalski, & Bond, 2008; Yoho, Popat, & Torres, 2014; Zacharoff et al., 2016). Genetic complementation
220 of each pathway has been demonstrated using a variety of extracellular electron acceptors (Chan et al.,
221 2015; Levar et al., 2014; Zacharoff et al., 2016).

222 Because it is difficult to measure the effective redox potential of metal (oxyhydr)oxides (Sander
223 et al., 2015), the redox potential of cultures undergoing active reduction of soluble Fe(III)-citrate was
224 first monitored for each strain (Figure 1). While the wild type reduced Fe(III) completely to Fe(II),
225 achieving a redox potential of -0.255 V vs. SHE, the Δ*cbcL* mutant strain (lacking the low-potential
226 system) was unable to reduce all Fe(III), and the redox potential only lowered to -0.15 V. The Δ*imcH*
227 mutant strain (lacking the high potential system) was unable to reduce Fe(III) when inoculated into the

228 high-potential environment. When both Δ*cbcL* and Δ*imcH* mutant strains were inoculated into the same
229 reactor, redox potential decreased with similar kinetics as the Δ*cbcL* strain, but continued on to a final
230 value similar to wild type. This was consistent with the Δ*cbcL* mutant strain first reducing Fe(III), until the
231 redox potential was low enough to be usable by the Δ*imcH* mutant. This hard transition from where the
232 Δ*cbcL* and Δ*imcH* mutant strains could actively reduce Fe(III) occurred in a range (between 0 and -0.1 V)
233 was similar to the theoretical potentials of many Fe(III)-(oxyhydr)oxides. With that observation that
234 these mutants behaved with Fe(III) citrate in a manner comparable to electrodes, we hypothesized that
235 mutants lacking the ImcH- and CbcL-dependent electron transfer pathways would respond similarly
236 when exposed to commonly used metal (oxyhydr)oxides.

237 **Here Figure 1**

238 **Evidence that the electron transfer pathway changes even in the absence of XRD-pattern changes**

239 Most Fe(III)-(oxyhydr)oxides do not exist at the high or low extremes represented by electrodes
240 or fresh Fe(III) citrate, but possess electron accepting potentials predicted to lie near the -0.10 V redox
241 potential threshold that requires a transition from ImcH-dependent to the CbcL-dependent reduction
242 pathways in electrode- and Fe(III)-citrate grown cells cells (Levar et al., 2014; Majzlan et al., 2004;
243 Majzlan, 2012; Thamdrup, 2000; Zacharoff et al., 2016). While testing this with electrodes or soluble
244 electron acceptors is straightforward, the redox potential of Fe(III)-(oxyhydr)oxides in this range is not
245 easy to predict or measure (Sander et al., 2015). Aging (accelerated by autoclaving or freeze drying) can
246 increase particle size and lower redox potential, or drive re-crystallization to lower redox potential forms
247 (Navrotsky et al., 2008; Roden, Urrutia, & Mann, 2000; Roden & Zachara, 1996; Roden, 2006; Thamdrup,
248 2000). As Fe(III)-(oxyhydr)oxide reduction is a proton consuming reaction (Kostka & Nealson, 1995;
249 Majzlan, 2012; Thamdrup, 2000), for each unit decrease in pH, the redox potential of the Fe(III)/Fe(II)

250 redox couple increases by ~59 mV per the Nernst equation (Bonneville, Van Cappellen, & Behrends,
251 2004; Kostka & Nealson, 1995; Majzlan, 2012; Thamdrup, 2000).

252 To test the hypothesis that *G. sulfurreducens* also utilizes ImcH- vs. CbcL-dependent pathways to
253 reduce minerals on the basis of redox potential, we prepared Fe(III)-(oxyhydr)oxides by slow
254 precipitation of $FeCl_3$ with NaOH (Lovley & Phillips, 1986), and characterized minerals before and after
255 addition to medium using powder XRD. While Fe(III)-(oxyhydr)oxides prepared in this manner are often
256 referred to as "poorly crystalline" or "amorphous", all XRD signatures of our slow-precipitation
257 preparations were consistent with akaganite (β-FeOOH) (Figure 2E). Because the β-FeOOH/Fe(II) redox
258 couple has a formal midpoint potential near -0.10 V vs. SHE (Majzlan, 2012), a fully oxidized suspension
259 of akaganeite would initially have a redox potential well above 0 V vs SHE, and theoretically require only
260 the 'high' potential pathway of *G. sulfurreducens*.

261 When wild-type, Δ*imcH,* and Δ*cbcL* strains were incubated with akaganeite that had not been
262 autoclaved (labeled as "Fresh"), wild-type cultures reduced the provided Fe(III)-(oxyhydr)oxide over the
263 course of 15 days. The Δ*cbcL* cultures containing the high-potential pathway initially reduced fresh
264 akaganeite at rates similar to wild type, but reduction slowed as Fe(II) accumulated, and the
265 concentration of Fe(II) never reached the extent of wild type. In contrast, Δ*imcH* cultures lacking the
266 high potential pathway demonstrated a substantial lag, remaining near background for 7 days (Figure
267 2A). Once metal reduction began, Δ*imcH* cultures were able to reach the final extent observed in wild
268 type. 14 day cell free controls did not exhibit any observable Fe(III)-(oxyhrdr)oxide reduction.

269 Medium containing akaganeite was then autoclaved, a treatment predicted to lower redox
270 potential due to accelerated aging. Both wild type and Δ*cbcL* performed similar to the fresh, un-
271 autoclaved sample, but the lag observed with Δ*imcH* was now much shorter, consistent with a lower
272 redox potential (Figure 2B). Despite the change in the Δ*imcH* Fe(III)-(oxyhydr)oxide reduction

273 phenotype, the XRD pattern before and after autoclaving was similar (Figure 2E). Such a lack of XRD
274 alteration in response to autoclaving has been previously noted (Hansel et al., 2015). This suggests that
275 phenotypic changes were due to mineral alteration outcomes not detected by powder XRD, such as
276 short-range structural order or particle aggregation, that lowered effective redox potential and allowed
277 growth of the Δ*imcH* strain lacking the high-potential pathway.

278 **Reduction phenotypes also respond to changes in medium pH that alter redox potential**

279 The lag in extracellular electron transfer by Δ*imcH*, in contrast to immediate reduction by Δ*cbcL,*
280 suggests that fresh akaganeite has an initial redox potential greater than -0.10 V vs. SHE. Based on this
281 hypothesis, after many days, a small amount of Fe(II) accumulates, and potential drops into a range
282 reducible by Δ*imcH*. If aging fresh akaganite by autoclaving shortened the lag in Figure 2B by lowering
283 redox potential, then manipulations designed to raise redox potential should extend this lag or prevent
284 Δ*imcH* from reducing akaganeite altogether.

285 When the pH of basal medium containing akaganeite was adjusted to 6.3 (raising the redox
286 potential ~30 mV (Kostka & Nealson, 1995; Majzlan, 2012; Thamdrup, 2000)), near complete inhibition
287 of reduction by Δ*imcH* was observed (Figure 2C). Autoclaving pH 6.3 akaganeite medium was not
288 sufficient to restore the reduction phenotype of Δ*imcH*, but it did aid reduction by Δ*cbcL* (Figure 2D). As
289 before, autoclaving at 6.3 did not substantially alter the XRD pattern of the mineral provided (Figure 2E).
290 Importantly, wild type, Δ*imcH,* and Δ*cbcL* grew without significant defects at pH values of 6.3 or 6.8 in
291 control experiments containing fumarate as the sole terminal electron acceptor (Table 1). Based on
292 these results, when akaganeite is autoclaved, the initial redox potential is likely lowered closer to -0.10 V
293 vs. SHE, permitting operation of the CbcL-dependent, low-potential pathway. Fresh akaganeite,
294 especially at pH 6.3, behaves consistent with a redox potential of 0 V or greater, thus preventing
295 reduction by cells containing only the low-potential pathway.

296 **Here Figure 2**

297 These two experiments, using aging to reduce redox potential and pH to raise redox potential,
298 caused changes in Δ*imcH* phenotypes that provided new evidence that *G. sulfurreducens* discriminates
299 between extracellular electron acceptors independent of the mineral properties accessed by powder
300 XRD. They also pointed to best practices for medium preparation in order to obtain consistent results if
301 the phenotype is sensitive to the redox potential of the environment. The amount of Fe(II) accumulated
302 after 7 days provided a repeatable readout of the ability of a *G. sulfurreducens* strain or mutant reduce a
303 given Fe(III)-(oxyhydr)oxide. According to this assay, the more Fe(II) produced in 7 days by an Δ*imcH*
304 mutant, the lower the initial redox potential of the mineral likely was.

305 **Other mineral forms consistent with a multiple-pathway model**

306 Additional Fe(III)-(oxyhydr)oxide minerals were then synthesized to test interactions of these
307 variables. When schwertmannite was synthesized using a rapid precipitation method (Regenspurg et al.,
308 2004), the mineral was stable at pH values below pH 4.0 and its structure could be confirmed by XRD.
309 However, abiotic transformation of schwertmannite to other mineral forms is accelerated at pH values
310 greater than 4.5 (Blodau & Knorr, 2006) and analysis of XRD patterns after schwertmannite was added
311 to *Geobacter* growth medium revealed rapid formation of XRD-amorphous minerals (Figure 3E), though
312 structural information may be elucidated with more powerful techniques such as synchrotron EXAFS.
313 Reduction phenotypes suggested this fresh mineral also produced a redox potential near 0 V vs. SHE, as
314 cells lacking the high potential pathway (Δ*imcH*) showed a lag at pH 6.8, which was shorter after the
315 mineral was autoclaved (Figure 3B). Reduction by Δ*imcH* was worst when the redox potential was
316 further raised by buffering to pH 6.3 (Figure 3C), while autoclaving pH 6.3 medium allowed a small
317 amount of Fe(II) accumulation that ended the lag after >8 days. These patterns with schwertmannite-
318 based minerals were similar to those observed with akaganite.

319 **Here Figure 3**

320 When Fe(III)-(oxyhrdr)oxide was prepared according to the 2-line ferrihydrite protocol of
321 Schwertmann and Cornell (2000), wild type and mutant phenotypes were again what was observed with
322 akaganite and schwertmannite. Freshly prepared mineral was reduced by Δ*cbcL* to within 67% of wild
323 type after seven days. When this mineral was aged by freeze drying (resulting in XRD-confirmed 2-line
324 ferrihydrite), reduction by Δ*cbcL* only 30% of wild type, suggesting that freeze drying lowered redox
325 potential of the mineral to a point where the low-potential pathway, encoded by *cbcL,* became more
326 important. Changing pH by 0.5 units was not sufficient to further alter reduction phenotypes, suggesting
327 that the freeze drying-aging process lowered the redox potential of ferrihydrite much more than 30 mV
328 of pH change could overcome.

329 A general trend emerged during these experiments, consistent with autoclaving, freeze drying,
330 and pH influencing redox potential in similar ways, regardless of the mineral. When reduction by Δ*imcH*
331 was near wild-type levels, reduction by Δ*cbcL* was typically at its lowest. When reduction by Δ*cbcL* was
332 near wild-type levels, Δ*imcH* cultures failed to reduce the provided electron acceptor. This trend
333 suggests that 1) the two mutants act as an *in vivo* sensor of initial redox potential, across a suite of
334 minerals, metals, and conditions, and 2) that both systems are employed by wild type bacteria
335 encountering these minerals under normal conditions.

336 Figure 4 represents all reduction data after seven days of incubation, from 17 different XRD-
337 characterized mineral forms performed in triplicate with three different strains, ranked according to
338 Δ*imcH* performance. Because redox potentials of these minerals can not directly measured, the order
339 shown in Figure 4 cannot be directly related to a quantitative measure of actual redox potential.
340 However, the data provides insight into how simple laboratory manipulations can affect experimental
341 outcomes, and how these are linked to redox potential changes.

342 For example, when Δ*imcH* mutants lacking the high potential pathway were unable to respire,
343 initial conditions were likely well above 0 V vs. SHE, such as with freshly precipitated minerals in medium
344 at pH 6.3. When exposed to the same high potential minerals, Δ*cbcL* mutants containing only the high
345 potential pathway were able to perform similar to wild type. As minerals were aged or manipulated to
346 lower their initial redox potential, the CbcL-dependent pathway became increasingly important to
347 achieve wild-type extents of reduction. These incubations highlighted the different contributions of
348 ImcH and CbcL to the initial rate vs. final extent of Fe(III) reduction, respectively.

349 Interestingly, some level of metal reduction was always observed for Δ*cbcL* mutants exposed to
350 minerals predicted to be very low potential acceptors. This result is similar to previous studies where
351 Δ*cbcL* still demonstrated a slow but detectable rate of respiration on electrodes poised at low redox
352 potentials (Zacharoff et al., 2016). This activity may reflect a yet-undiscovered pathway used under
353 thermodynamically challenging conditions, where neither ImcH- nor CbcL-dependent pathways can
354 function.

355 The results in Figure 4 represent a suite of well-understood minerals (2-line ferrihydrite,
356 goethite, akaganeite, schwertmannite, and birnessite), in which variability is typically introduced
357 through freeze-drying, autoclaving, and pH adjustments. These variables alter mineral crystal structure,
358 particle size, degree of aggregation, surface area, and surface charge, and thus influence microbial
359 attachment or behavior in unpredictable ways (Cutting, et al., 2009; Majzlan et al., 2004; Navrotsky et
360 al., 2008; Roden, 2006). However, these manipulations change redox potential in predictable ways.
361 Based on the overall pattern of responses, we propose that redox potential is a master variable affecting
362 the pathway of extracellular electron acceptor reduction used by *G. sulfurreducens*.

363 **Here Figure 4**

364 **Cells lacking the CbcL-dependent pathway have increased growth yield.**

365 A key question stemming from this work relates to the evolutionary forces selecting for multiple
366 electron transfer pathways at the inner membrane. As cells lacking the ImcH-dependent pathway are
367 often able to completely reduce a provided mineral after a small amount of Fe(II) accumulates, why not
368 encode a single electron transfer pathway and allow it operate at all potentials, thus eliminating the
369 need to encode pathways controlling respiration across multiple redox potential windows? One
370 hypothesis is that the multiple pathways encoded *G. sulfurreducens* are able to take advantage of the
371 different amounts of energy represented by the spectrum of metal (oxyhydr)oxides, by more efficiently
372 conserving these energy differences.

373 To test this hypothesis, the cell yield of *G. sulfurreducens* strains in which one pathway was
374 removed was measured. Because Δ*cbcL* can initially reduce akaganeite, direct comparisons were
375 possible when a low inoculum of each strain was added to medium containing this mineral (autoclaved
376 at pH 6.8, as in Figure 2B) and incubated. In all experiments, Δ*cbcL* generated more colony forming units
377 per mol Fe(II) produced than wild type *G. sulfurreducens*. For each mM of Fe(III) reduced, Δ*cbcL*
378 produced 2.5 ± 0.3 x 10^6 CFU, while wild type produced 0.8 ± 0.1 and 1.6 ± 0.1 x 10^6 CFU, respectively
379 (n=5 for each strain) (Figure 5A). These results indicated that when electron flow was forced through the
380 ImcH-dependent pathway (as in Δ*cbcL*), more cells were produced per Fe(III) reduced.

381 Cell attachment to mineral particles could confound plate counts in experiments with cells
382 grown on solid particles. In a second series of experiments, medium containing acetate and fumarate
383 was inoculated with cultures at the same stage of akaganeite reduction. Because all wild-type and
384 mutant cultures grow at similar rates with fumarate as the electron acceptor (see Table 1), the point at
385 which optical density is detectable is a function of the number of cells in the inoculum. In all of these
386 experiments, Δ*cbcL* again demonstrated significantly more cells per mol Fe(II) reduced than wild type.

387 Yield was also measured after a small inoculum of wild type or Δ*cbcL* cells were allowed to
388 reduce Fe(III)-citrate, and cells were harvested and washed free of soluble iron (which can affect the
389 BCA assay). The Δ*cbcL* cultures again had a significantly increased protein yield (Figure 5B). When
390 standardized to the amount of Fe(II), the yield of cells forced to use only the ImcH pathway was 170% of
391 the wild type using both pathways during complete reduction of Fe(III).

392 Combined with previous data showing that cells using ImcH-dependent pathways support faster
393 growth rates (Zacharoff et al., 2016), this supports the hypothesis that *G. sulfurreducens* alters its
394 electron transfer pathway to obtain a higher yield per electron transferred. These data indicate that
395 these electron transfer pathways are able to switch 'on' and 'off' in response to changing redox
396 potential of external electron acceptors. This provides one possible explanation for the complexity and
397 burden associated with encoding multiple pathways of electron transfer across the inner membrane.

398 **Here Figure 5**

399 **Discussion:**

400 Fe(III)-(oxyhydr)oxide minerals in nature exist as a complex continuum of potential energies. As
401 such, it is unsurprising that bacteria would evolve equally complex mechanisms able to harness the
402 energy available during respiration to these metals. While a single pathway essential for reduction of all
403 metals emerged in the model metal-reducing *Shewanella spp.,* a similarly simple solution remained
404 elusive in *Geobacter spp.*. The data reported here demonstrates that even under the most common
405 laboratory conditions where Fe(III)-(oxyhydr)oxide is precipitated and added to medium, *G.*
406 *sulfurreducens* will utilize multiple electron transfer pathways to accomplish what is considered to be
407 wild-type levels of Fe(III) reduction. For Fe(III)-(oxyhydr)oxides that are predicted to have redox
408 potentials around 0 V, such as schwertmannite, akaganeite, and ferrihydrite, the electron-accepting
409 potential decreases as Fe(II) accumulates, and triggers utilization of electron transfer pathways that
410 support lower cell yield and slower growth rate, but still allow some respiration. The ability of *G.*
411 *sulfurreducens* to respond to the changing redox potential of its environment likely allows this organism
412 to make the most efficient use of the provided mineral.

413 Based on proteomic studies, *G. sulfurreducens* expresses at least 78 multiheme *c*-type
414 cytochromes under different laboratory conditions, yet mutant analyses were initially unable to link
415 particular cytochromes to reduction of specific extracellular electron acceptors (Aklujkar et al., 2013;
416 Leang et al., 2003, 2010; Rollefson et al., 2009, 2011; Shi et al., 2007). One hypothesis for cytochrome
417 diversity that drives such -omic comparisons is that separate pathways will exist based on solubility
418 (chelated vs. oxide) or metal (Fe vs. Mn). However, despite their many physiochemical differences,
419 Fe(III)-citrate and Mn(IV)-(oxyhydr)oxides both represent high potential acceptors, from the viewpoint
420 of the inner membrane, and our data suggest that this variable influences at least one portion of the
421 electron transfer pathway. As we detect evidence for at least one other pathway in this work, and the *G.*
422 *sulfurreducens* genome appears to encode at least 4 other inner membrane quinone oxidoreductases,

423 redox potential differences may help to explain additional complexity of *Geobacter.* Possessing protein
424 machinery able extract the full advantage from minerals as they descend through the redox tower also
425 helps explain the dominance of these metal-reducing organisms in contaminated subsurface
426 environments undergoing rapid redox potential changes.

427 In order to characterize and biochemically dissect extracellular electron transfer in dissimilatory
428 metal reducing organisms such as *G. sulfurreducens*, closer attention may need to be paid not just to
429 crystal structure, but the actual redox potential experienced by the organisms. Commonly synthesized
430 Fe-(oxyhydr)oxides prepared by precipitation of Fe(III) can produce very different rates of reduction or
431 mutant phenotypes depending on the age of the material and the length of time one is willing to
432 incubate cells. A distinction between initial rates of Fe(III)-(oxyhydr)oxide reduction, where higher-
433 potential conditions exist, and final extent of reduction achieved by slower but lower potential pathways
434 may help separate these confounding effects. As Fe(II) begins to accumulate during the course of Fe(III)-
435 (oxyhydr)oxide reduction by metal reducing microorganisms, the redox potential will change as the ratio
436 of Fe(II)/Fe(III) changes and as mineral structure is altered in response in increased Fe(II) concentration.
437 One would also expect significant differences in washed cell suspensions, where the degree of
438 respiratory coupling to growth is not part of the assay, since electron flow through the ImcH- and CbcL-
439 dependent pathways support different growth rates and yields.

440 It now appears that in *G. sulfurreducens* a transition from an ImcH-dependent electron transfer
441 pathway to a CbcL-dependent pathway occurs both when electrodes and commonly used Fe(III)-
442 (oxyhydr)oxides are provided as sole terminal electron acceptors. The initial rate and total extent of
443 Fe(III)-(oxyhydr)oxide reduction may also be the result of a series of redox potential dependent
444 processes in environmental samples, with each step supporting different cell yields. Competition in the
445 environment could occur along any part of this continuum, rewarding those capable of rapid growth

446 when the Fe(III)-(oxyhydr)oxide is high potential, or those able to survive with electron acceptors at
447 relatively low redox potentials. The prevalence of ImcH and CbcL homologues in other dissimilatory
448 metal reducing organisms and in metagenomics data from sites undergoing active metal reduction
449 (Levar et al., 2014; Zacharoff et al., 2016) suggests that this type of redox discrimination could also occur
450 in diverse organisms, and provides opportunities for further exploration of redox potential dependent
451 respiration in these organisms and their environments.

452

453 **Acknowledgements:**

454 C.E.L. was supported by the State of Minnesota's MNDrive program, D.R.B. was partially
455 supported by the Office of Naval Research grant N000141210308, A.J.D was supported by UMN U.R.O.P,
456 and C.L.H and B.M.T were supported by the State of Minnesota's L.C.C.M.R program.

457

458 **References:**

459 Aklujkar, M. A., Coppi, M. V, Leang, C., Kim, B. C., Chavan, M. A., Perpetua, L. A., … Holmes, D. E. (2013).
460 Proteins involved in electron transfer to Fe(III) and Mn(IV) oxides by *Geobacter sulfurreducens* and
461 *Geobacter uraniireducens*. *Microbiology*, *159*, 515–535.

462 Blodau, C., & Knorr, K. H. (2006). Experimental inflow of groundwater induces a "biogeochemical regime
463 shift" in iron-rich and acidic sediments. *Journal of Geophysical Research: Biogeosciences*, *111*, 1–
464 12.

465 Bonneville, S., Van Cappellen, P., & Behrends, T. (2004). Microbial reduction of iron(III) oxyhydroxides:
466 Effects of mineral solubility and availability. *Chemical Geology*, *212*, 255–268.

467 Caccavo, F., Lonergan, D. J., Lovley, D. R., Davis, M., Stolz, J. F., & McInerney, M. J. (1994). *Geobacter*
468 *sulfurreducens sp. nov*., a hydrogen- and acetate-oxidizing dissimilatory metal-reducing
469 microorganism. *Applied and Environmental Microbiology*, *60*, 3752–3759.

470 Chan, C. H., Levar, C. E., Zacharoff, L., Badalamenti, J. P., & Bond, D. R. (2015). Scarless genome editing
471 and stable inducible expression vectors for *Geobacter sulfurreducens*. *Applied and Environmental*
472 *Microbiology*, *82*

473 Cutting, R. S., Coker, V. S., Fellowes, J. W., Lloyd, J. R., & Vaughan, D. J. (2009). Mineralogical and
474 morphological constraints on the reduction of Fe(III) minerals by *Geobacter sulfurreducens.*
475 *Geochimica et Cosmochimica Acta*, *73*, 4004–4022.

476 Flynn, T. M., O'Loughlin, E. J., Mishra, B., DiChristina, T. J., & Kemner, K. M. (2014). Sulfur-mediated
477 electron shuttling during bacterial iron reduction. *Science*, *344*, 1039–1042.

478 Green, J., & Paget, M. S. (2004). Bacterial redox sensors. *Nature Reviews. Microbiology*, *2*, 954–966.

479 Hansel, C. M., Lentini, C. J., Tang, Y., Johnston, D. T., Wankel, S. D., & Jardine, P. M. (2015). Dominance of
480 sulfur-fueled iron oxide reduction in low-sulfate freshwater sediments. *The ISME Journal*, *9*, 2400-
481 2412.

482 Kostka, J. E., & Nealson, K. H. (1995). Dissolution and reduction of magnetite by bacteria. *Environmental*
483 *Science & Technology*, *29*, 2535–40.

484 Leang, C., Coppi, M. V, & Lovley, D. R. (2003). OmcB, a *c*-type polyheme cytochrome, involved in Fe(III)
485 reduction in *Geobacter sulfurreducens*. *Journal of Bacteriology*, *185*, 2096–2103.

486 Leang, C., Qian, X., Mester, T., & Lovley, D. R. (2010). Alignment of the *c*-type cytochrome OmcS along
487 pili of *Geobacter sulfurreducens*. *Applied and Environmental Microbiology*, *76*, 4080–4084.

488 Levar, C. E., Chan, C. H., Mehta-Kolte, M. G., & Bond, D. R. (2014). An inner membrane cytochrome
489 required only for reduction of high redox potential extracellular electron acceptors. *mBio*, *5*,
490 e02034-14.

Lovley, D. R., & Phillips, E. J. (1986). Organic matter mineralization with reduction of ferric iron in anaerobic sediments. *Applied and Environmental Microbiology*, *51*, 683–689.

Lovley, D. R., & Phillips, E. J. (1987). Rapid assay for microbially reducible ferric iron in aquatic sediments. *Applied and Environmental Microbiology*, *53*, 1536–1540.

Majzlan, J. (2011). Thermodynamic stabilization of hydrous ferric oxide by adsorption of phosphate and arsenate. *Environmental Science & Technology*, *45*, 4726–32.

Majzlan, J. (2012). Minerals and Aqueous Species of Iron and Manganese as Reactants and Products of Microbial Metal Respiration. In J. Gescher & A. Kappler (Eds.), *Microbial Metal Respiration; From Geochemistry to Potential Applications* (1st ed., pp. 1–28). Springer.

Majzlan, J., Navrotsky, A., & Schwertmann, U. (2004). Thermodynamics of iron oxides: Part III. Enthalpies of formation and stability of ferrihydrite ($\sim Fe(OH)_3$), schwertmannite ($\sim FeO(OH)_{3/4}(SO4)_{1/8}$), and ε-$Fe_2O_3$. *Geochimica et Cosmochimica Acta*, *68*, 1049–1059.

Marsili, E., Rollefson, J. B., Baron, D. B., Hozalski, R. M., & Bond, D. R. (2008). Microbial biofilm voltammetry: direct electrochemical characterization of catalytic electrode-attached biofilms. *Applied and Environmental Microbiology*, *74*, 7329–7337.

Michel, F. M., Ehm, L., Antao, S. M., Lee, P. L., Chupas, P. J., Liu, G., … Parise, J. B. (2007). The structure of ferrihydrite, a nanocrystalline material. *Science*, *316*, 1726–1729.

Navrotsky, A., Mazeina, L., & Majzlan, J. (2008). Size-driven structural and thermodynamic complexity in iron oxides. *Science*, *319*, 1635–1638.

Nealson, K. H., & Myers, C. R. (1992). Microbial reduction of manganese and iron: New approaches to carbon cycling. *Applied and Environmental Microbiology*, *58*, 439–443.

Nealson, K. H., & Saffarini, D. (1994). Iron and manganese in anaerobic respiration: environmental significance, physiology, and regulation. *Annual Review of Microbiology, 48*, 311-343.

Orsetti, S., Laskov, C., & Haderlein, S. B. (2013). Electron transfer between iron minerals and quinones: estimating the reduction potential of the Fe(II)-goethite surface from AQDS speciation. *Environmental Science & Technology*, *47*, 14161–14168.

Post, J. E., & Veblen, D. R. (1990). Crystal structure determinations of synthetic sodium, magnesium, and potassium birnessite using TEM and the Rietveld method. *American Mineralogist*, *75*, 477–489.

Raven, K. P., Jain, A., & Loeppert, R. H. (1998). Arsenite and arsenate adsorption on ferrihydrite: Kinetics, equilibrium, and adsorption envelopes. *Environmental Science and Technology*, *32*, 344–349.

Regenspurg, S., Brand, A., & Peiffer, S. (2004). Formation and stability of schwertmannite in acidic mining lakes. *Geochimica et Cosmochimica Acta*, *68*, 1185–1197.

Roden, E. E. (2006). Geochemical and microbiological controls on dissimilatory iron reduction. *Comptes Rendus Geoscience*, *338*, 456–467.

Roden, E. E., Urrutia, M. M., & Mann, C. J. (2000). Bacterial Reductive Dissolution of Crystalline Fe (III) Oxide in Continuous-Flow Column Reactors, *Applied and Environmental Microbiology, 66*, 1062–1065.

Roden, E. E., & Zachara, J. M. (1996). Microbial Reduction of Crystalline Iron(III) Oxides: Influence of Oxide Surface Area and Potential for Cell Growth. *Environmental Science & Technology*, *30*, 1618–1628.

Rollefson, J. B., Levar, C. E., & Bond, D. R. (2009). Identification of genes involved in biofilm formation and respiration via mini-*Himar* transposon mutagenesis of *Geobacter sulfurreducens*. *Journal of Bacteriology*, *191*, 4207–4217.

Rollefson, J. B., Stephen, C. S., Tien, M., & Bond, D. R. (2011). Identification of an extracellular polysaccharide network essential for cytochrome anchoring and biofilm formation in *Geobacter sulfurreducens*. *Journal of Bacteriology*, *193*, 1023–1033.

Russell, J. B., & Cook, G. M. (1995). Energetics of bacterial growth: balance of anabolic and catabolic reactions. *Microbiological Reviews*, *59*, 48–62.

Sander, M., Hofstetter, T. B., & Gorski, C. A. (2015). Electrochemical analyses of redox-active iron minerals: A review of non-mediated and mediated approaches. *Environmental Science & Technology*, *49*, 5862–5878.

Schwertmann, U., & Cornell, R. M. (2000). *Iron Oxides in the Laboratory: Preparation and Characterization* (2nd ed.). Wiley-VCH Verlag GmbH.

Shi, L., Squier, T. C., Zachara, J. M., & Fredrickson, J. K. (2007). Respiration of metal (hydr)oxides by *Shewanella* and *Geobacter*: a key role for multihaem *c*-type cytochromes. *Molecular Microbiology*, *65*, 12–20.

Thamdrup, B. (2000). Bacterial manganese and iron reduction in aquatic sediments. In B. Schink (Ed.), *Advances in Microbial Ecology* (16th ed., pp. 41–84). Springer.

Thauer, R. K., Jungermann, K., & Decker, K. (1977). Energy conservation in chemotrophic anaerobic bacteria. *Bacteriological Reviews*, *41*, 100-180.

Yoho, R. A., Popat, S. C., & Torres, C. I. (2014). Dynamic potential-dependent electron transport pathway shifts in anode biofilms of *Geobacter sulfurreducens*. *ChemSusChem*, 7*,* 3413-3419.

Zacharoff, L., Chan, C. H., & Bond, D. R. (2016). Reduction of low potential electron acceptors requires the CbcL inner membrane cytochrome of *Geobacter sulfurreducens*. *Bioelectrochemistry*, *107,* 7-13.

556 **Figure 1**

557 ***Redox potential controls the behavior of Δ*imcH *and Δ*cbcL *mutants*:** Redox potential was recorded in real time
558 during reduction of Fe(III)-citrate by each culture. Cells lacking the CbcL-dependent pathway (Blue trace) initially
559 reduced Fe(III), but could not lower the redox potential below -0.15 V vs SHE. Cells lacking the ImcH-dependent
560 pathway (Red trace) could not lower the redox potential from the uninoculated value (+0.04 V vs SHE). The redox
561 potential was lowed to the same point as wild type (black trace) when a co-inoculum of the two mutants was used
562 (Green trace). Traces are representative of at least triplicate experiments for each strain or co-culture.

563 **Figure 2**

564 ***Autoclaving and changing pH alters mutant phenotypes.*** In all cases, wild type is represented by black circles,
565 Δ*cbcL* by downward pointing blue triangles, and Δ*imcH* by upward pointing red triangles. (A) A long lag is observed
566 for Δ*imcH* inoculated into medium with no autoclaving ("Fresh"). (B) The lag observed for Δ*imcH* is decreased
567 when the medium is aged through autoclaving. (C) Decreasing the pH by 0.5 units eliminates akaganeite reduction
568 by Δ*imcH*. (D). Aging pH 6.3 medium through autoclaving is not sufficient to decrease the redox potential enough
569 to allow for reduction by Δ*imcH*. All data shown are the mean and standard deviation for triplicate cultures, and
570 are representative of at least duplicate incubations. (E) XRD patterns of the mineral used in panels A-D. The XRD
571 pattern for the mineral prior to addition to medium and autoclaving ("Untreated") is also shown.

572 **Figure 3**

573 ***Addition of schwertmannite to growth medium at pH 6.3 or pH 6.8 alters mineralogy, and mutant behavior*:**
574 Rapid precipitation of an Fe sulfide solution with hydrogen peroxide yields XRD-pure schwertmannite ("untreated",
575 Panel E), but when this mineral suspension is added to growth medium, abiotic transformation is observed.
576 Autoclaving these media lead to further mineral transformation. Treatments aimed at raising and lowering redox
577 potential affected reduction by *ΔimcH* mutants similar to results seen in Figure 2.

578 **Figure 4**

579 **G. sulfurreducens *requires both ImcH and CbcL for complete reduction of a range of minerals:*** Cultures of Δ*imcH*
580 (red upward pointing triangles) and Δ*cbcL* (blue downward pointing triangles) were incubated with minerals as the
581 sole terminal electron acceptor, and the extent of Fe(II) or Mn(II) accumulation was measured relative to that of
582 wild type *G. sulfurreducens*. Data shown are the mean and standard deviation of triplicate cultures. Conditions are
583 ordered left to right in order of Δ*imcH* reduction, from best to worst. Akaganeite, β-FeOOH. Schwertmannite,
584 $Fe_8O_8(OH)_6(SO_4)\cdot nH_2O$. 2-line Fh (Ferrihydrite), ca. $Fe_{10}O_{14}(OH)_2$. Birnessite $Na_xMn_{2-x}(IV)Mn(III)_xO_4$, x ~ 0.4,
585 Goethite, α-FeOOH.

586 **Figure 5**

587 ***Δ*cbcL *has an increased growth yield when respiring extracellular electron acceptors:*** Removal of the CbcL-
588 dependent pathway increases the growth yield compared to wild type for two different electron acceptors. (A) For
589 wild-type and Δ*cbcL* strains reducing akaganeite (Autoclaved at pH 6.8, as in Figure 3B) as the sole terminal
590 electron acceptor, Δ*cbcL* generated more cells per unit Fe(II) produced than did wild type. (B) Δ*cbcL* produced
591 more protein per unit Fe(II) produced than wild type when reducing Fe(III)-citrate as the sole terminal electron
592 acceptor. These data suggest that electron flow through ImcH supports conservation of more energy, when high

593 potential electron acceptors reducible by this system are available. Each data point (Black circles=wild type, blue
594 triangles=Δ*cbcL*) represents an individual culture and bars are the mean and standard deviation of the data shown.

595

596

597

Table 1

Strain	Source	Doubling time in minimal medium at different pH (hours)*	
		6.3	6.8
Geobacter sulfurreducens			
Wild type (ATCC 51573)	Caccavo et al., 1994	6.5±0.2	5.6±0.2
Δ*cbcL*	Zacharoff et al., 2016	5.6±0.2	6.4±0.1
Δ*imcH*	Chi Ho Chan et al., 2015	5.7±0.1	6.0±0.2

* Doubling times are the mean and standard deviation of at least two idependent experiments of triplicate cultures

Figure 1

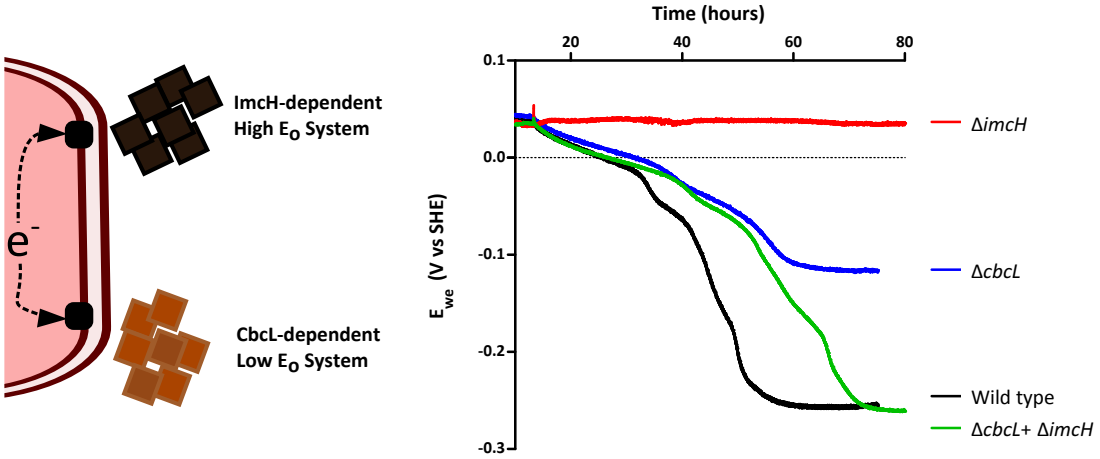

***Redox potential controls the behavior of* Δ**imcH** *and* Δ**cbcL** *mutants*:** Redox potential was recorded in real time during reduction of Fe(III)-citrate by each culture. Cells lacking the CbcL-dependent pathway (Blue trace) initially reduced Fe(III), but could not lower the redox potential below -0.15 V vs SHE. Cells lacking the ImcH-dependent pathway (Red trace) could not lower the redox potential from the uninoculated value (+0.04 V vs SHE). The redox potential was lowed to the same point as wild type (black trace) when a co-inoculum of the two mutants was used (Green trace). Traces are representative of at least triplicate experiments for each strain or co-culture.

Figure 2

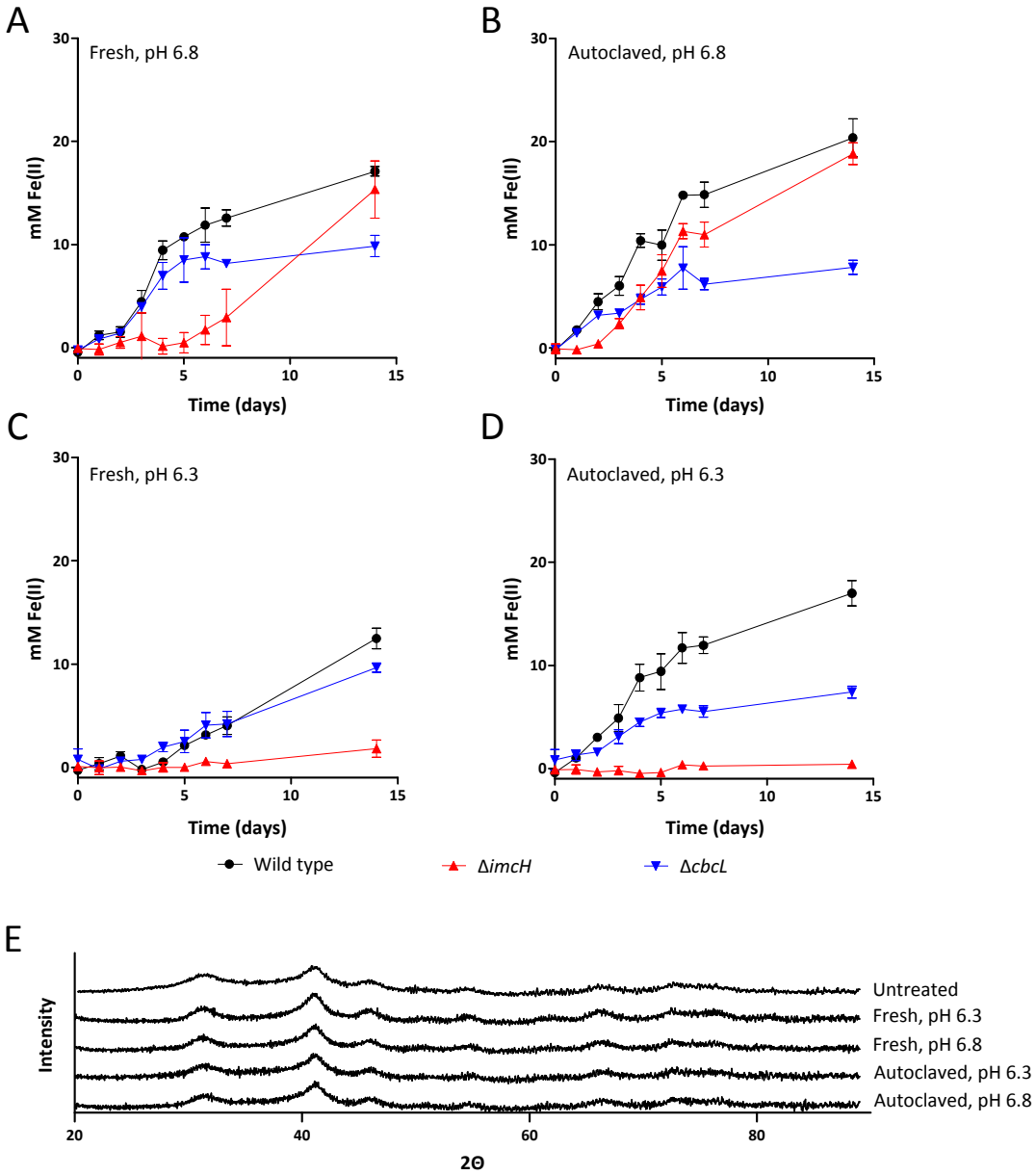

Autoclaving and changing pH alters mutant phenotypes: In all cases, wild type is represented by black circles, Δ*cbcL* by downward pointing blue triangles, and Δ*imcH* by upward pointing red triangles. (A) A long lag is observed for Δ*imcH* inoculated into medium with no autoclaving ("Fresh"). (B) The lag observed for Δ*imcH* is decreased when the medium is aged through autoclaving. (C) Decreasing the pH by 0.5 units eliminates akaganeite reduction by Δ*imcH*. (D). Aging pH 6.3 medium through autoclaving is not sufficient to decrease the redox potential enough to allow for reduction by Δ*imcH*. All data shown are the mean and standard deviation for triplicate cultures, and are representative of at least duplicate incubations. (E) XRD patterns of the mineral used in panels A-D. The XRD pattern for the mineral prior to addition to medium and autoclaving ("Untreated") is also shown.

Figure 3

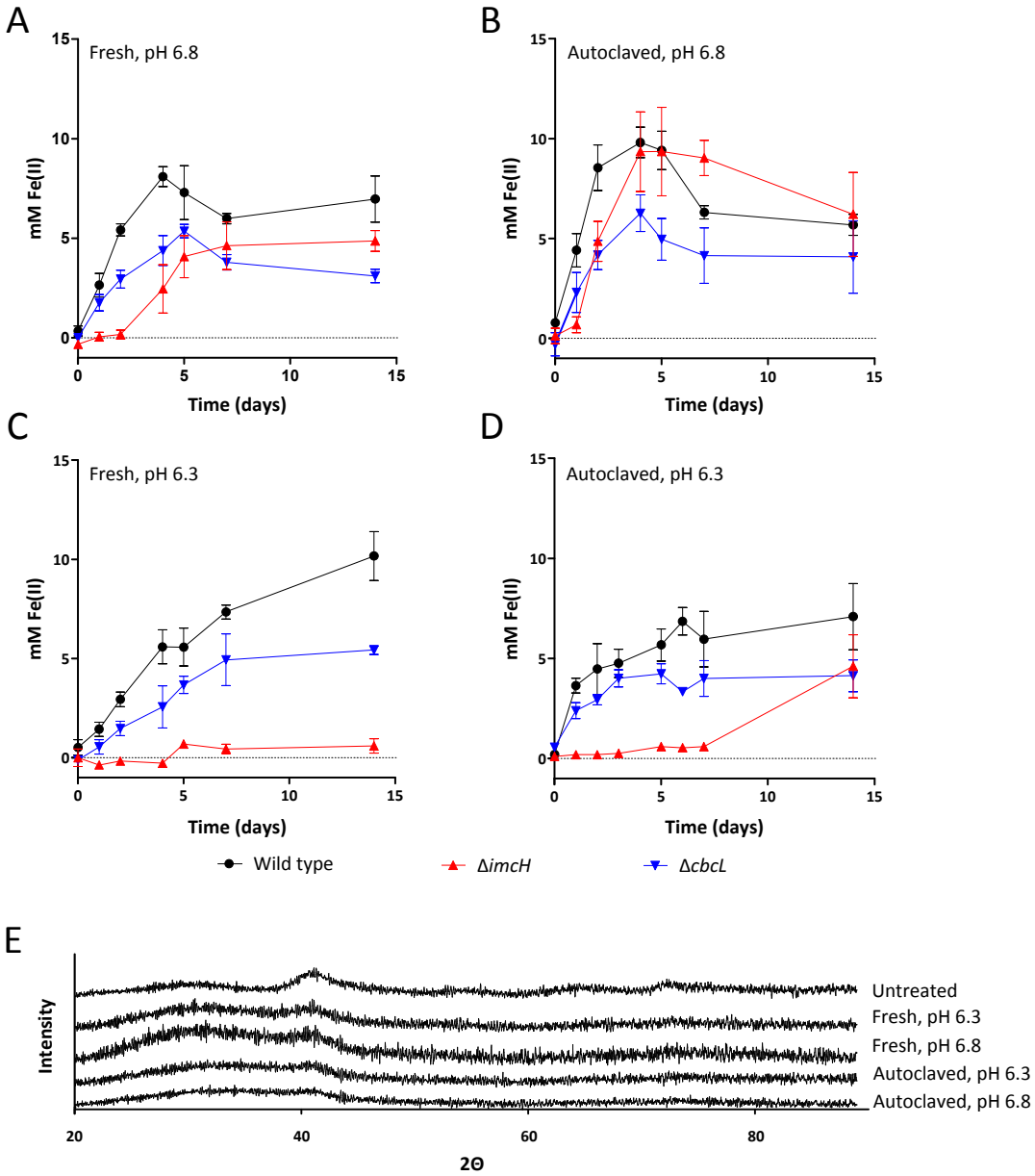

Addition of schwertmannite to growth medium at pH 6.3 or pH 6.8 alters mineralogy, and mutant behavior: Rapid precipitation of an Fe sulfide solution with hydrogen peroxide yields XRD-pure schwertmannite ("untreated", Panel E), but when this mineral suspension is added to growth medium, abiotic transformation is observed. Autoclaving these media lead to further mineral transformation. Treatments aimed at raising and lowering redox potential affected reduction by *ΔimcH* mutants similar to results seen in Figure 2.

Figure 4

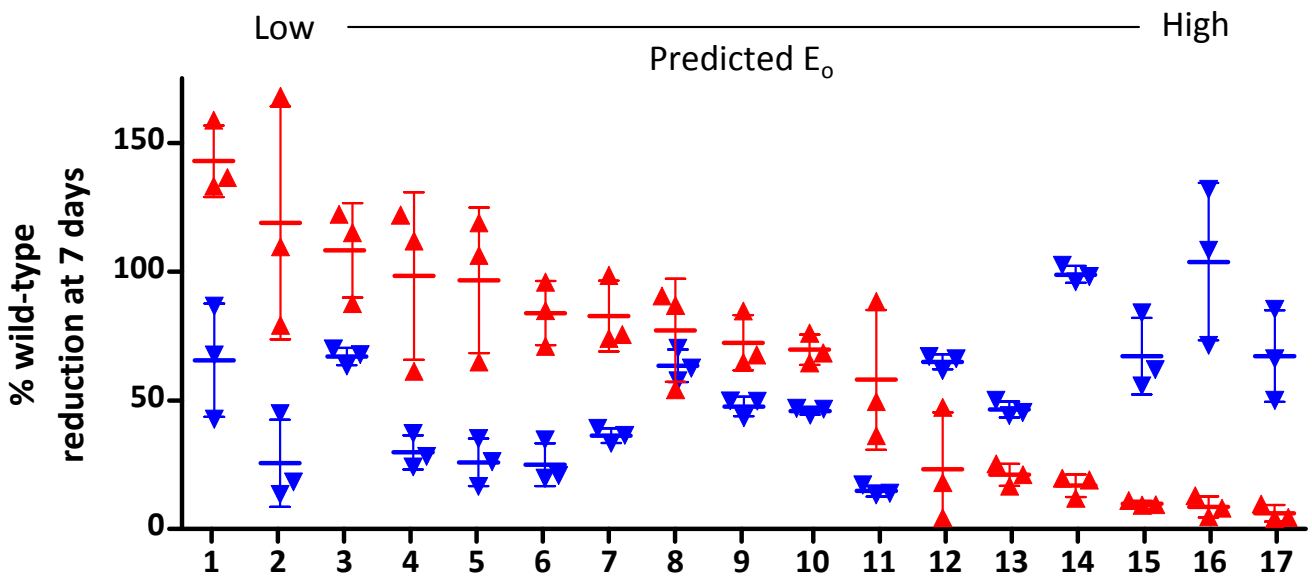

#	Starting mineral*	Freeze dried (Y/N)	Autoclaved (Y/N)	pH	Resulting mineral[†]
1	Schwertmannite	N	Y	6.8	XRD Amorphous
2	2-line Fh	Y	N	6.3	2-line Fh
3	2-line Fh	N	N	6.8	Akaganeite
4	Goethite	Y	N	6.8	Goethite
5	2-line Fh	Y	N	6.8	2-line Fh
6	2-line Fh	Y	Y	6.3	2-line Fh
7	Akaganeite	N	Y	6.8	Akaganeite
8	Schwertmannite	N	N	6.8	XRD Amorphous
9	Akaganeite	N	Y	6.6	Akaganeite
10	Akaganeite	N	Y	6.5	Akaganeite
11	2-line Fh	Y	Y	6.8	2-line Fh
12	Akaganeite	N	N	6.8	Akaganeite
13	Akaganeite	N	Y	6.3	Akaganeite
14	Birnessite	N	N	6.8	Birnessite
15	Schwertmannite	N	Y	6.3	XRD Amorphous
16	Akaganeite	N	N	6.3	Akaganeite
17	Schwertmannite	N	N	6.3	XRD Amorphous

*Listed mineral is mineral identity prior to treatment with media or autoclaving.

[†]Listed mineral is mineral identity after treatmeant with media or autoclaving and before innoculation with *G. sulfurreducens*

G. sulfurreducens *requires both ImcH and CbcL for complete reduction of a range of minerals:* Cultures of Δ*imcH* (red upward pointing triangles) and Δ*cbcL* (blue downward pointing triangles) were incubated with minerals as the sole terminal electron acceptor, and the extent of Fe(II) or Mn(II) accumulation was measured relative to that of wild type *G. sulfurreducens*. Data shown are the mean and standard deviation of triplicate cultures. Conditions are ordered left to right in order of Δ*imcH* reduction, from best to worst. Akaganeite, β-FeOOH. Schwertmannite, $Fe_8O_8(OH)_6(SO_4)\cdot nH_2O$. 2-line Fh (Ferrihydrite), ca. $Fe_{10}O_{14}(OH)_2$. Birnessite $Na_xMn_{2-x}(IV)Mn(III)_xO_4$, x ~ 0.4, Goethite, α-FeOOH.

Figure 5

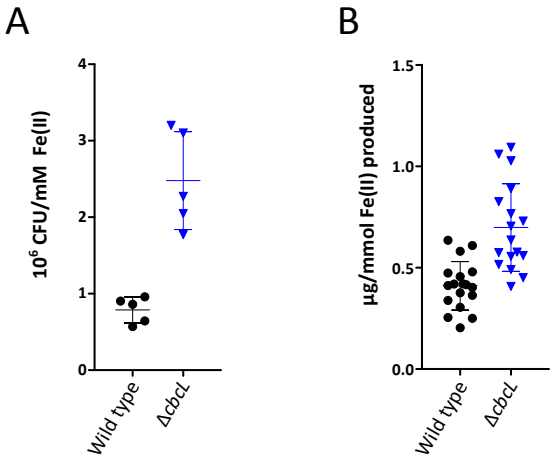

Δ*cbcL *has an increased growth yield when respiring extracellular electron acceptors: Removal of the CbcL-dependent pathway increases the growth yield compared to wild type for two different electron acceptors. (A) For wild-type and Δ*cbcL* strains reducing akaganeite (Autoclaved at pH 6.8, as in Figure 3B) as the sole terminal electron acceptor, Δ*cbcL* generated more cells per unit Fe(II) produced than did wild type. (B) Δ*cbcL* produced more protein per unit Fe(II) produced than wild type when reducing Fe(III)-citrate as the sole terminal electron acceptor. These data suggest that electron flow through ImcH supports conservation of more energy, when high potential electron acceptors reducible by this system are available. Each data point (Black circles=wild type, blue triangles=Δ*cbcL*) represents an individual culture and bars are the mean and standard deviation of the data shown.